

Power-Electronic Transformer Tap-Changer for Increased AC Arc Furnace Productivity

A. Korn^{*}, P. K. Steimer^{*}, Y. Suh^{**} and J. W. Kolar⁺

^{*}) ABB Ltd. Power Electronics and MV Drives, 5300 Turgi, Switzerland

^{**}) Chonbuk National University, Chonju, Korea

⁺) Swiss Federal Institute of Technology - ETH

Power Electronics Systems Laboratory, 8092 Zürich, Switzerland

E-mail contact: arthur.korn@ch.abb.com

Abstract – The productivity of AC electric arc smelters widely used in the nonferrous metals industry is related to the arc voltage. Attempts to improve productivity with longer arcs and higher arc voltages give rise to power fluctuations which cause voltage flicker and frequent arc reignition failures. The furnace power is commonly regulated by moving the electrode rods to adjust the arc length. A 100 MW AC arc furnace power supply equipped with semiconductor switched regulation windings which greatly enhance furnace power control bandwidth is presented, along with suitable winding arrangements, semiconductor topologies, harmonic filters and commutation methods. This system was simulated together with a Cassie-Mayr dynamic arc model. The simulation model as well as the four-step commutation sequence has been experimentally verified by building and testing a single phase 230 V, 2 kW PWM modulated tap-changer. The simulations and experiments demonstrate that power-electronic transformer tap-changers with the ratings necessary for AC arc furnace power supplies are within reach of current semiconductor technology. They are significantly more effective at AC arc furnace power regulation in terms of device rated power than controlled series reactor approaches.

I. INTRODUCTION

Electric smelting furnaces are widely used in the metals industry. They provide melting and reaction energy to a bath of liquid metal by means of an electric current, DC or AC. DC furnaces are built with two electrodes, one is a rod lowered through the furnace cover, the other one is built into the hearth. AC furnaces do not use a hearth electrode but three or six rod electrodes. AC smelters are cheaper to build and maintain than DC smelters and are consequently much more widely used [3]. The power of AC electric arc smelters is commonly regulated by mechanical adjustments to the arc length and the transformer transmission ratio.

Operation at higher arc voltages improves the productivity of the furnace, as the output is tightly related to the furnace power while the current is responsible for cost factors such as the conductor, bushing and cooling system size, energy losses and electrode wear.

The arc voltage is increased by operating with longer arcs; however this also increases arc power fluctuations which cannot be compensated for by the slow mechanical adjustments in use. In extremis such fluctuations cause arc reignition failures, followed by periods of asymmetric furnace operation associated with reduced power and unbalance stresses on neighboring electricity consumers and generators. The power fluctuations also put strain on the hydraulic electrode regulation used for power regulation in present plants and cause voltage flicker.

By improving the furnace power regulation, the flicker can be reduced and the arc voltage increased, reducing operating costs by lowering wear and grid disturbances.

II. FURNACE POWER REGULATION

Power regulation aims to maintain a certain power in the presence of disturbances. This situation can be represented by the circuit shown in Fig. 1 where a constant power load is fed by a fixed voltage feed and a regulation voltage source in series to the two. As the regulation device should have a neutral power balance, a shunt source is added which balances the power of the series regulation source without canceling its effect.

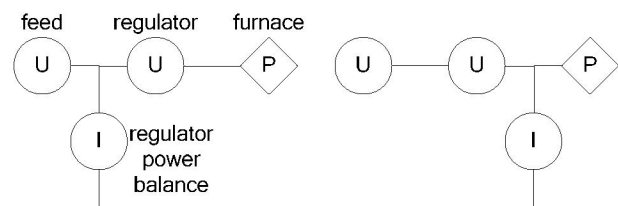


Fig. 1. Circuits considered to calculate the regulation power demand for load power regulation. Feed side recuperation (left) and load side recuperation (right).

When the regulation power is recuperated on the feed side of the series source, the load voltage is

$$U_{load} = U_{feed} - \frac{S_{series}}{I_{series}} = U_{feed} - \frac{S_{series} U_{load}}{P_{load}} = \frac{U_{feed}}{1 + \frac{S_{series}}{P_{load}}} \quad (1)$$

If the recuperation is done on the load side of the series source, the load voltage is

$$U_{load} = U_{feed} - \frac{S_{series}}{I_{series}} = U_{feed} - \frac{S_{series} U_{load}}{P_{load} - S_{series}} \quad (2)$$

$$= U_{feed} \left(1 + \frac{S_{series}}{P_{load}} \right)$$

These functions are plotted in Fig. 2 which shows the regulator power rating necessary to achieve a certain voltage change of the load in relation to the load power. A voltage range of $\pm 10\%$ is expected to be sufficient for power regulation. It follows that a regulation device using active power can achieve a $\pm 10\%$ voltage range with merely $\pm 10\%$ power while a device based on reactive power would need 83% power.

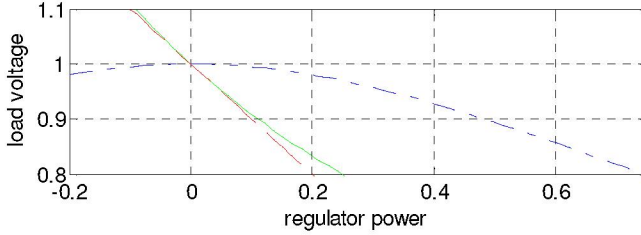


Fig. 2. Constant power load voltage regulation with a series voltage source using either active power (feed side recuperation solid green, load side recuperation dashed red) or reactive power (blue dash-dotted).

Recently, SPLC, a thyristor controlled series reactor based furnace regulation device has been introduced, which successfully reduces flicker [2] but requires large and expensive series inductors. The SmoothArc concept uses diacs, which are believed to deteriorate arc stability due to the prolonged current zero-crossing [3]. Both approaches constitute adjustable series reactors.

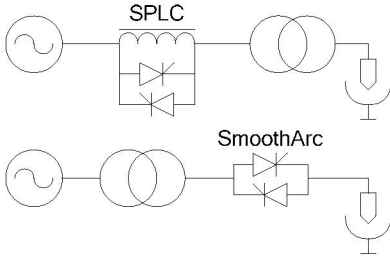


Fig. 3. Variable reactance topologies proposed for AC arc furnace regulation. The reactive power compensation is not shown.

The adjustable series voltage source restricted to active power with a power balancing shunt current source corresponds to an adjustable ideal transmission and can be realized as an adjustable transformer. The voltage and current

transmission ratios of transformers are proportional to the ratio of the number of turns in each winding. Hence the transmission ratio can be modified by changing the number of turns in a winding. In the simplest case, one of several leads connected to different places on a winding (so called taps) can be connected to the external terminal by a switch (the tap-changer).

III. POWER-ELECTRONIC TAP-CHANGER

Various winding and switch arrangements for power-electronic tap-changers have been proposed but there is no obvious figure of merit to compare them [7][8]. Considering the total built in switch and winding powers, the maximum required blocking voltage of the switches along a current path (as a measure for the forward voltage and thus of conduction loss) and the number of available transmission ratios, it becomes evident that series connections of regulation windings without taps and switch arrangements which permit reversal of the windings in the circuit as shown in Fig. 5 are preferable to structures with taps. Adding taps cannot reduce the required blocking voltage rating of the switches connected between the outermost terminals, irrespective of the arrangement, while the built-in winding power and the maximum blocking voltage along a current path are not affected. Adding transmission ratios by series connecting regulation windings with a constant total number of turns does neither affect the overall installed switch power nor the forward voltage [1] however.

For continuous adjustments of the transmission ratio the switch on the winding with the least turns is pulse width modulated. The remaining switches are only actuated at current zero-crossing and can thus be thyristors. The number of series connected regulation windings and therefore the number of turns on the smallest winding (which determines the blocking voltage of PWM modulated gate-turn off semiconductors) is a degree of freedom for cost optimization.

As both the current and voltage polarities on all switches do reverse, four-quadrant switches have to be used. To guarantee that only safe switch to diode and diode to switch commutations occur, a four-step commutation sequence as known in the context of matrix converters [15] is applied. In [5] it is claimed that a DC voltage component will occur at the transformer (driving it towards saturation) with voltage oriented four-step commutation as the actual commutation takes place either after two or three steps, depending on instantaneous power flow direction. However, a DC current was neither observed in simulations nor in laboratory experiments.

Flying capacitor AC choppers [12] were considered for the PWM switch but the control of the flying capacitor voltage was found to be infeasible at switching frequencies of less than 1.2 kHz per stage which are suitable for high-power gate turn-off semiconductors such as IGCTs.

IV. MODULATION

The arc voltage contains over 10% fifth and seventh harmonics. The tap changer cannot be used as an active harmonic filter due to the low switching frequencies of power semiconductors with the necessary current ratings. PWM modulation with a carrier frequency of six times the line frequency and a single carrier for all three phases is thus being used, causing harmonics for which filters have to be present anyway. A single harmonic could be turned into a common mode by using a separate phase-shifted carrier per phase [1]. As the tap changer harmonics are only a fraction of the harmonics caused by the arc load, the simpler solution of using a single carrier is preferred.

V. ARC ELECTRIC MODEL

The arc's electric behavior can be described by the Cassie-Mayr model [3]:

$$\dot{i}_{arc} = \frac{r_{arc}}{\tau} \left(1 - \frac{u_{arc} i_{arc}}{P_0} \right) \quad (3)$$

where r_{arc} is the instantaneous arc resistance, u_{arc} and i_{arc} are the arc voltage and current respectively, P_0 is the typical arc power loss and τ the time constant of the arc resistance. Yongjoong Lee determined the model parameters for a 1 kV arc to be: $P_0 = 10^6$ W and $\tau = 600$ μ s.

For the implementation in PLECS a controlled voltage source was driven by a Simulink implementation of the logarithm of the equation above, which is numerically favorable:

$$u_{arc} = i_{arc} e^{\rho}, \dot{\rho} = \frac{1}{\tau} \left(1 - \frac{i_{arc}^2}{P_0} e^{2\rho} \right) \quad (4)$$

This model does not explain all power fluctuations observed in AC arc furnaces, thus the closed loop control of those fluctuations cannot be adequately simulated.

VI. TRANSFORMER

A transformer model shall be derived with the aim to operate the arc model presented above at 100 MW (three phase). The transformer needs a rating of approximately 125 MVA due to the reactive power consumption of the arc. Transformers in this power range have stray inductances of about 10%. The nominal transformer secondary voltage necessary to achieve the desired furnace power of 100 MW was determined using simulations of the Cassie-Mayr arc model with series elements representing the transformer, busbar and electrode stray inductances and resistances and was found to be $\hat{U}_{load} = 1.9$ kV. The operating point range, load losses and magnetization current were chosen to correspond with a furnace transformer operated in Baoshan, China. Hence, the lowest secondary voltage in the control range will be $\check{U}_{load} = 1900 \text{ V} \cdot 689.6 \text{ V} / 1203 \text{ V} = 1090 \text{ V}$. Around

every operating point in this control range, the electronic tap changer shall have at least $p = 20\%$ (i.e. $\pm 10\%$) voltage range.

A combination of a single electronic tap-changer stage in series with a mechanical tap-changer is considered for the simulation as shown in Fig. 5. The transmission ratio of the electromechanical tap-changer is $U_{base} = \alpha U_{load}$, the transmission ratio of the electronic regulation winding is $U_{tap} = \beta U_{load}$. The hybrid tap changer has a variable α with the bounds $\check{\alpha} \leq \alpha \leq \hat{\alpha}$.

The maximum voltage across the electronic tap-changer is proportional to β :

$$\hat{U}_{tap} = \beta \hat{U}_{load} (1 + p/2) \quad (5)$$

The electronic regulation range has to be sufficient at both ends of the control range:

$$\begin{aligned} U_{feed} / (\check{\alpha} - \beta) &= \hat{U}_{load} (1 + p/2) \\ U_{feed} / (\check{\alpha} + \beta) &\leq \hat{U}_{load} (1 - p/2) \\ U_{feed} / (\hat{\alpha} - \beta) &\geq \check{U}_{load} (1 + p/2) \\ U_{feed} / (\hat{\alpha} + \beta) &= \check{U}_{load} (1 - p/2) \end{aligned} \quad (6)$$

β shall be minimized. The first and second inequalities imply

$$\beta \geq U_{feed} / 2 / \hat{U}_{load} \frac{p}{1 - p^2/4} \quad (7)$$

the third and fourth ones imply

$$\beta \geq U_{feed} / 2 / \check{U}_{load} \frac{p}{1 - p^2/4} \quad (8)$$

Because $\hat{U}_{load} > \check{U}_{load}$ the second constraint implies the first and β is chosen to satisfy it to equality:

$$\begin{aligned} \beta &= \frac{U_{feed}}{2\check{U}_{load}} \frac{p}{1 - p^2/4} \\ \check{\alpha} &= \frac{U_{feed}}{\hat{U}_{load}} \frac{1}{1 + p/2} + \beta \\ \hat{\alpha} &= \frac{U_{feed}}{\check{U}_{load}} \frac{1}{1 - p/2} - \beta \end{aligned} \quad (9)$$

The maximum voltage across the electronic tap-changer in this hybrid scheme is then:

$$\hat{U}_{tap} = \frac{U_{feed}}{2} \frac{\hat{U}_{load}}{\check{U}_{load}} \frac{p}{(1 - p/2)} \quad (10)$$

Focusing the simulation model to the PWM modulated tap changer, only a three port transformer has to be modeled. The other switches are assumed to be fixed at the highest power positions. The nominal transmission ratio of the high power port to the secondary side is $\check{\alpha} - \beta$, from the low power port it is $\check{\alpha}$.

For simulation and analysis at frequencies below any transformer resonances and with linear magnetization, such a

transformer can be represented as a series connection of a mutual inductance and a mutual resistance:

$$\vec{u} = L \frac{\partial \vec{i}}{\partial t} + R \vec{i} \quad (11)$$

L and R are symmetric matrices due to the reciprocity of linear time invariant inductors and resistors.

The listed load losses of the Baoshan transformer are about 0.6% of to the maximum rated power. 0.1% are assumed to be dissipated on the load side. The resistance of the low power winding is calculated assuming the primary side winding resistances are proportional to the turn number.

$$\begin{aligned} R_1 &= 0.005 \frac{U_{feed}^2}{S} \\ R_2 &= R_1 \frac{\tilde{\alpha} - \beta}{\tilde{\alpha}} \\ R_3 &= 0.001 \frac{\tilde{U}_{load}^2}{S} \end{aligned} \quad R = \begin{pmatrix} R_1 & R_2 & 0 \\ R_2 & R_2 & 0 \\ 0 & 0 & R_3 \end{pmatrix} \quad (12)$$

The no load magnetizing current of 0.15% defines the open circuit inductances, which are the diagonal elements of the inductance matrix. The wye-delta transformer also has a transmission ratio due to the connection, which is taken into account by dividing α and β by $\sqrt{3}$. The short circuit inductance from the high power terminal to the load terminal is 10%. The inductance $L_{sc,hl}$ among the taps was estimated to be 1% in the feed side units. The short circuit inductance from the lower power terminal to the load terminal is calculated assuming that the short circuit inductance is proportional to the square of the turn count.

$$\begin{aligned} L_{oc,h} &= 1/0.0015 \frac{U_{feed}^2}{S\omega} & L_{sc,hs} &= 0.1 \frac{U_{feed}^2}{S\omega} \\ L_{oc,l} &= \frac{(\tilde{\alpha} - \beta)^2}{\tilde{\alpha}^2} \frac{U_{feed}^2}{S\omega} & L_{sc,ls} &= \frac{(\tilde{\alpha} - \beta)^2}{\tilde{\alpha}^2} L_{sc,hs} \\ L_{oc,s} &= 1/0.0015 \frac{\tilde{U}_{load}^2}{S\omega} & L_{sc,hl} &= 0.01 \frac{U_{feed}^2}{S\omega} \end{aligned} \quad (13)$$

The off-diagonal elements can be calculated by solving eq. 11 (neglecting the resistance for convenience) for a short-circuit on port y measured from port x which yields:

$$L_{x,y} = \sqrt{\left(L_{x,x} - \frac{\|U_x\|}{\|I_x\|} \right)} L_{y,y} \quad (14)$$

So far the windings on a single leg of the transformer have been considered. To expand the model to a three phase transformer, the above model was used in each phase separately. The magnetic coupling between phases can be ignored if no common mode currents can flow (as is the case when delta windings are used or the neutral point is isolated) and therefore the fluxes in the legs always sum up to zero.

VII. FILTER DESIGN

The large harmonic content in the arc voltage calls for effective filters. Determining factors for filter selection are the type of the harmonic source, the order of the harmonic to be attenuated and the need for reactive power.

Harmonic voltage sources require high input impedance filters to avoid harmonic currents between source and filter. Complementary low input impedance filters are needed with harmonic current sources [14]. Resonant filters are more suitable than low-pass filters for low order harmonics as they are not limited to 20dBm/decade attenuation per filter order, at the expense of a separate filter for each harmonic. The filters should not worsen the power factor. Shunt filters always provide capacitive reactive power and are usually dimensioned to compensate an inductive load. Series resonant filters act as series inductors at fundamental frequency, consuming a load dependent amount of reactive power. Low-pass filters both provide a fixed amount of reactive power and consume load dependent reactive power.

At the tap, the tap-changer and the regulation winding represent harmonic current sources, accordingly the circuit placed there needs to have low impedance to harmonic and high frequencies. A shunt capacitor is a simple and effective solution, it was dimensioned to compensate the reactive power of the load at the maximum power operating point and thus to minimize the maximum switch current. The tuning was done in simulations with the nonlinear Cassie-Mayr arc model to get a realistic picture of the reactive power consumption of the arc.

Towards the line the tap-changer behaves as a harmonic voltage source as the transformer impedance at the high power port is approximately the short circuit impedance from there to the tap where the harmonics meet low impedance. Therefore the feeding circuit needs to have high impedance at harmonic frequencies. Parallel resonant series filters tuned to the fifth and seventh harmonic are placed here to achieve the necessary attenuation of these strong low order harmonics. They are dimensioned around 1% reactors, leading to values of $C_{f5} = 400\%$ and $C_{f7} = 204\%$. The capacitors seem large in the feed's units, scaling their ratings to the actually occurring voltages of under 20% reduces the ratings by a factor of $0.2^2 = 0.04$ to reasonable values of $C_{f5} = 16\%$ and $C_{f7} = 8.2\%$.

The reactive power consumed by the parallel resonant series filters is eventually compensated using a series resonant shunt filter tuned to the eleventh harmonic. Using a resonant filter instead of a capacitor has the advantage that the resonance frequency can be adjusted.

VIII. SIMULATION RESULTS

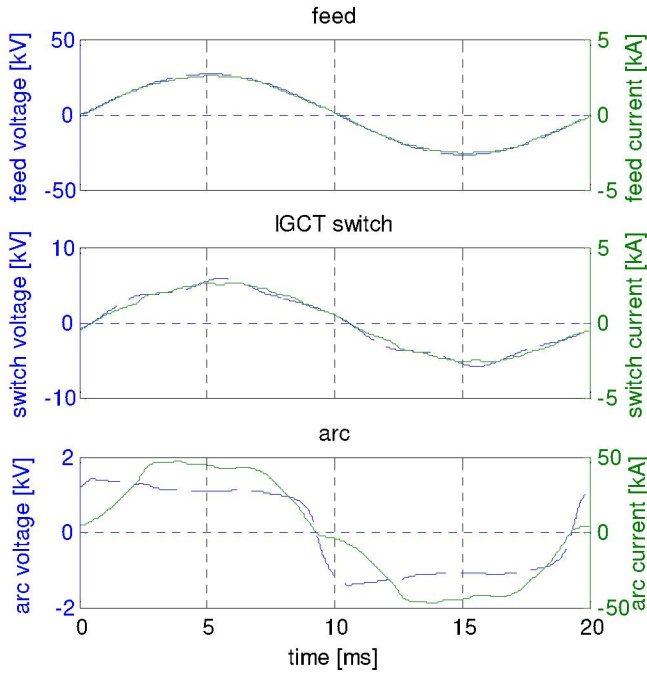


Fig. 4. Simulation results for voltage (dashed) and current (solid) in a single phase at the feed, the IGCT changeover switch and the arc load.

The simulation model of the circuit shown in Fig. 5 encompasses the tap-changer, filters, tapped transformer and arc load and includes the semiconductor losses in the PWM modulated stage.

The tap changer is modeled as an ideal switch in the electrical model, each semiconductor's average loss power is calculated as the sum of the conduction loss power $P_{cond} = R_t \text{avg}(I^2) + V_{to} \text{avg}(I)$ and the switching loss power averaged over all switchings $P_{sw} = T^{-1} \sum E_{sw, norm} S_{sw}$. The normalized switching loss energy $E_{sw, norm}$ for IGCT turn-off, turn-on or diode turn-off is selected from a look-up table and denormalized by the switched power for each turn-off or turn-on.

At the PWM modulated switch a fundamental frequency peak voltage of 5.2 kV and a peak current of 2.5 kA are expected. Two paralleled Mitsubishi FGC1500A-130DS RB-IGCTs have suitable current turn-off and blocking voltage ratings of 1.5 kA and 6.5 kV. At the highest power operating point of 100 MW furnace power (0.48 duty cycle) the hottest junction has a temperature of 110°C at 40°C ambient temperature, which is acceptable. The efficiency of 96.6% from feed to arc does not include any inductor iron or conduction losses. The feed current THD (ratio of amplitudes) is 1.9%.

Some traces are shown in Fig. 4. The semiconductor ratings can be chosen close to the fundamental frequency components' peak values due to the small harmonic content of the switch voltage and current.

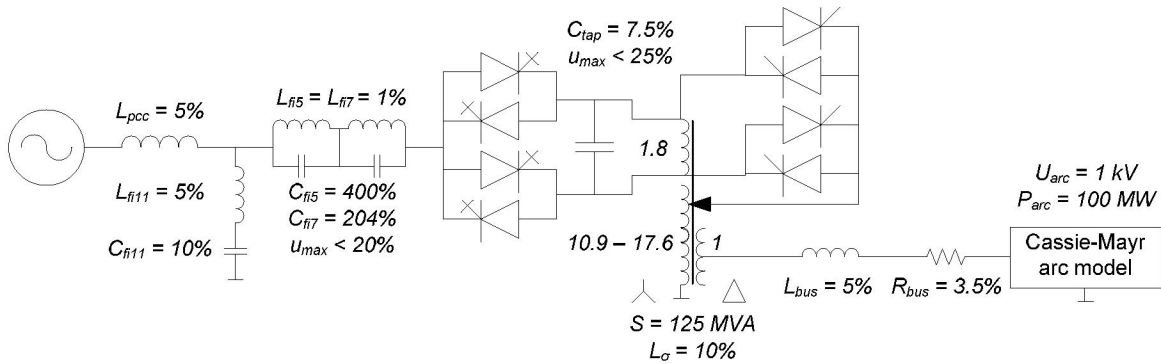


Fig. 5. Single-line diagram of the proposed 100MW electronically regulable AC arc smelter power supply.

IX. PWM TAP-CHANGER LAB EXPERIMENT

A single-phase 230 V, 2 kW, 1.2 kHz power-electronic tap-changer was built as shown in Fig. 6 and the experimental results compared to simulations in order to verify the transformer model and to test the four-step commutation.

A voltage oriented four-step commutation sequence was implemented as a state machine (also shown in Fig. 6) on the PLD of a standard ABB converter control board PP D116

with a commutation time-step of 21 μ s. The voltage polarity is detected by a comparator isolated from the power circuit by an isolation amplifier. The polarity is only considered at the beginning of the commutation sequence, this will never lead to overcurrents as the worst case snubber capacitor voltage reached by the time the last transition is executed is $\sin(2 \cdot \pi \cdot 50\text{Hz} \cdot 3 \cdot 21\mu\text{s}) = 2\% \approx 6.5\text{V}$, which is less than the nominal forward voltages of the six semiconductor elements in the short circuit.

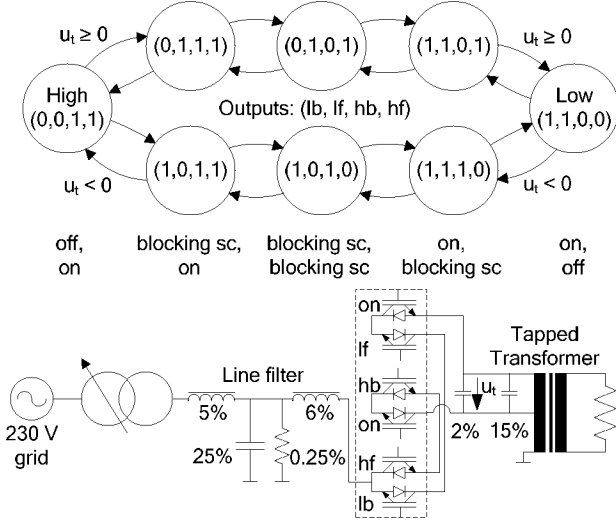


Fig. 6. Schematic and commutation logic of the laboratory set-up used for the verification of the tapped transformer modelling approach and the commutation method.

The four-quadrant switches were built using a LoPak5 IGBT module containing three half-bridges in one package. The module is designed such that the stray inductance between the terminals normally used to connect the DC link is minimized. Consequently the commutation path of the tap changer also uses only those terminals as shown in Fig. 6. The third IGBT present in each four-quadrant switch is always turned on. The connections were all made with insulated wire for the sake of simplicity and to keep the stray inductance of the commutation path small by keeping the conductors close together.

No diode snubbers were installed as the IGBTs are rated for 1.2 kV which proved to be far sufficient when the set-up was initially operated with gradually increasing feed voltage. Fig. 8 shows a turn-off transient recorded at the highest current occurring in normal operation of the setup.

The desaturation monitoring circuit of the gate drive requires the collectors of the upper IGBTs (with respect to a DC link) to be externally connected and had to be disabled, just as the upper-lower interlocking logic which would interfere with the commutation sequence and does not serve its purpose with the topology used.

The laboratory experiment was built around an existing transformer, thus measurements could be taken to parametrize the transformer simulation model. The inductance matrix was derived from the nominal voltage ratios, an open circuit and three short circuit measurements. The diagonal elements are determined by the open circuit inductance of one winding (magnetization inductance) and the nominal voltage ratios between windings, the off diagonal elements are derived from the short circuit measurements using eq. 14.

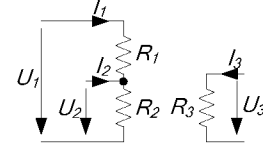


Fig. 7. Simplified model of the resistances in the transformer used for the identification of the resistivity matrix R .

The elements of the transformer resistance matrix for the simulation model have been determined from DC resistance measurements assuming a simplified equivalent circuit which only considers the winding resistances as shown in Fig. 7 such that R becomes:

$$R = \begin{pmatrix} R_1 + R_2 & R_2 & 0 \\ R_2 & R_2 & 0 \\ 0 & 0 & R_3 \end{pmatrix} \quad (15)$$

R_1 , R_2 and R_3 can now be determined from three open circuit DC resistance measurements, one per terminal, yielding the diagonal elements of the matrix. The skin and proximity effects are not considered, thus this model is not ideal for loss calculations.

The higher switching frequency permitted to use a low-pass filter which could be put together with readily available spare components. The harmonic attenuation and the reactive power compensation are not optimal however.

Simulation traces and experimental measurements are shown in Fig. 9 The low frequency harmonics in the line current observed experimentally are also present when the tap-changer is not switching at all and are thus thought to be caused by line voltage harmonics. The switching transients are benign, no excessive over-voltages or -currents occur.

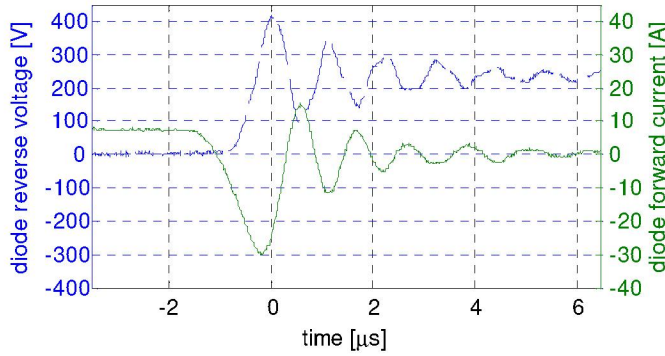


Fig. 8. Switching transient recorded in the laboratory at 90% duty-cycle. Diode reverse voltage (dashed, left scale) and diode forward current (solid, right scale).

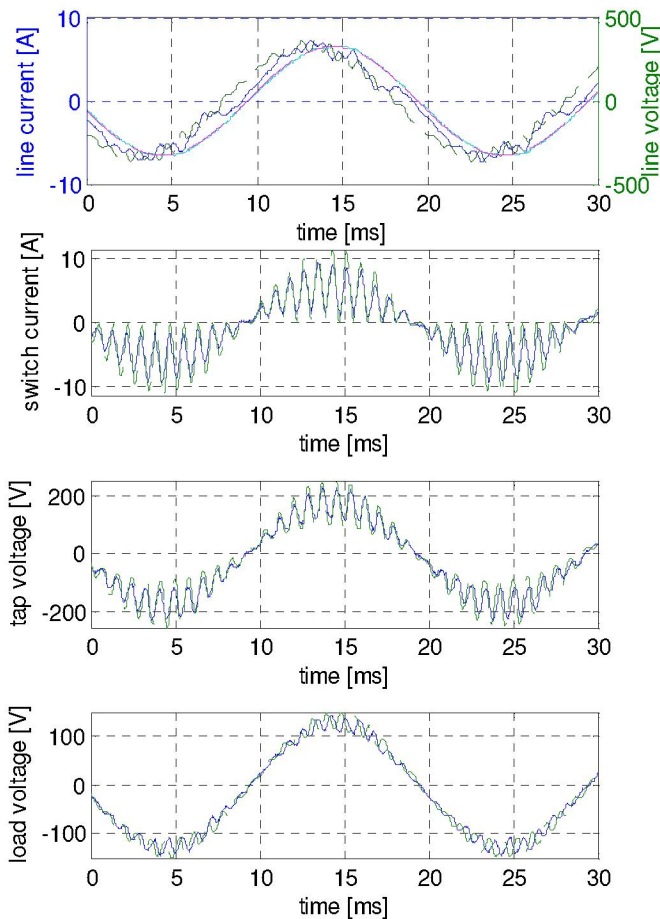


Fig. 9. Measured (solid) and simulated (dashed) traces of the experiment recorded at 50% duty cycle.

X. CONCLUSION

The presented simulation and experiment demonstrate that power-electronic transformer tap-changers with ratings in the range of tens of megawatts as necessary for furnace power supplies are within reach of current semiconductor technology. They are substantially more effective at AC arc

furnace power regulation in terms of device rated power than TCSR.

Parallel resonant series filters have been shown to provide good attenuation of the current harmonics induced by the arc load and the tap changer.

The four-step commutation method has successfully been applied to an experimental PWM modulated tap changer. The good agreement between simulation and experiment confirms the presented modeling method for tapped transformers.

REFERENCES

- [1] A. Korn, P. Steimer, Y. Suh and D. Aggeler, "Power-Electronic Transformer Tap-Changers for Fast AC Arc Furnace Power Control," M.S. thesis, PES, ETH and ABB, Zurich, 2008
- [2] T. Gerritsen, T. Ma, M. Sedighy, J. Janzen, F. Stober, N. Voermann, and J.R. Frias, „SPLC – a power supply for smelting furnaces,” presented at the International Laterite Nickel Symposium, 2004.
- [3] Y. Lee, H. Nordborg, Y. Suh, and P. Steimer, "Arc stability criteria in AC arc furnace and optimal converter topologies," in *22nd Annu. IEEE Applied Power Electronics Conf.*, 2007, pp. 1280–1286.
- [4] D. Divan and J. Sastry, "Controllable Network Transformers," in *IEEE Power Electronics Specialists Conf.*, 2008, pp. 2340-2345.
- [5] P. Bauer and R. Schoevaars, "Bidirectional switch for a solid state tap changer," in *IEEE Power Electronics Specialists Conf.*, 2003, vol. 1, pp. 466–471.
- [6] O. Demirci, D.A. Torrey, R.C. Degeneff, F.K. Schaeffer and R.H. Frazer, "A new approach to solid-state on load tap changing transformers," *IEEE Trans. Power Deliv.*, vol. 13, pp. 952–961, Jul. 1998.
- [7] J. Faiz and B. Siahkollah, "New solid-state onload tap-changers topology for distribution transformers," *IEEE Trans. Power Deliv.*, vol. 18, pp. 136–141, Jan. 2003.
- [8] E.A. Gomez and B.D. Monroy, "Solid-state tap changers: New configurations and applications," *IEEE Trans. Power Deliv.*, vol. 22, pp. 2228–2235, Oct. 2007.
- [9] D.-H. Jang and G.-H. Choe, "Step-up/down ac voltage regulator using transformer with tap changer and PWM AC chopper," *IEEE Trans. Ind. Electron.*, vol. 45, pp. 905–911, Dec. 1998.
- [10] B.K. Johnson and G. Venkataramanan, "A hybrid solid state phase shifter using PWM AC converters," *IEEE Trans. Power Deliv.*, vol. 13, pp. 1316–1321, Oct. 1998.
- [11] G.G. Karady and P. Parihar, "Integrated PWM and transformer switching technique for AC voltage regulation," in *APEC 1994 Conf. Proc.*, 1994, vol. 2, pp. 961–967.
- [12] E. Lefevre, T. Meynard, and P. Viarouge, "Robust two-level and multilevel PWM AC choppers," presented at the European Power Electronics and Devices Conf., Graz, Austria, 2001.
- [13] L.A.C. Lopes, G. Joos, and Boon-Teck Ooi, "A high-power PWM quadrature booster phase shifter based on a multimodule AC controller," *IEEE Trans. Power Electron.*, vol. 13, pp. 357–365, Mar. 1998.
- [14] F.Z. Peng and D.J. Adams, "Harmonic sources and filtering approaches-series/parallel, active/passive, and their combined power filters," in *Conf. Rec. IEEE Ind. Appl. Conf.*, vol. 1, pp. 448–455, 1999.
- [15] P.W. Wheeler, J. Rodriguez, J.C. Clare, L. Empringham and A. Weinstein, "Matrix converters: a technology review," *IEEE Trans. Ind. Electron.*, vol. 49, pp. 276–288, Apr. 2002.